Author(s): Mikkilä, Joona & Eskelinen, Antti-Pekka & Niemelä, Elina H. & Linko, Veikko & Frilander, Mikko J. & Törmä, Päivi & Kostiainen, Mauri A.

Title: Virus-Encapsulated DNA Origami Nanostructures for Cellular Delivery

Year: 2014

Version: Post print

Please cite the original version:

Mikkilä, Joona & Eskelinen, Antti-Pekka & Niemelä, Elina H. & Linko, Veikko & Frilander, Mikko J. & Törmä, Päivi & Kostiainen, Mauri A. 2014. Virus-Encapsulated DNA Origami Nanostructures for Cellular Delivery. Nano Letters. Volume 14, Issue 4. 2196-2200. ISSN 1530-6984 (printed). DOI: 10.1021/nl500677j.

Virus Encapsulated DNA Origami Nanostructures for Cellular Delivery

*Joona Mikkilä[1,4], Antti-Pekka Eskelinen[2], Elina H. Niemelä[3], Veikko Linko[1], Mikko J. Frilander[3], Päivi Törmä[2], Mauri A. Kostiainen[4]**

[1] Molecular Materials, Department of Applied Physics, Aalto University, FI-00076 Aalto, Finland

[2] COMP Centre of Excellence, Department of Applied Physics, Aalto University, FI-00076 Aalto, Finland

[3] Institute of Biotechnology, University of Helsinki, FI-00014 Helsinki, Finland

[4] Biohybrid Materials, Department of Biotechnology and Chemical Technology, Aalto University, FI-00076 Aalto, Finland

KEYWORDS: DNA nanotechnology, self-assembly, virus capsid protein, cellular delivery, cell uptake

ABSTRACT: DNA origami structures can be programmed into arbitrary shapes with nanometer scale precision, which opens up numerous attractive opportunities to engineer novel functional materials. One intriguing possibility is to use DNA origamis for fully tunable, targeted and triggered drug delivery. In this communication, we demonstrate the coating of DNA origami nanostructures with virus capsid proteins for enhancing cellular delivery. Our approach utilizes purified cowpea chlorotic mottle virus capsid proteins that can bind and self-assemble on the origami surface through electrostatic interactions and further pack the origami nanostructures inside the viral capsid. Confocal microscopy imaging and transfection studies with a human HEK293 cell line indicate that protein coating improves cellular attachment and delivery of origamis into the cells by 13-fold compared to bare DNA origamis. The presented method could readily find applications not only in sophisticated drug delivery applications but also in organizing intracellular reactions by origami-based templates.

DNA origami technique enables the formation of arbitrary, exact and complex two- and three-dimensional nano-objects with custom twists, curvatures and tension.[1–8] Traditionally, origamis are formed by folding a scaffold strand, i.e. a long single-stranded DNA (ssDNA), into desired shape with the help of a predefined set of oligonucleotides, but recently also scaffold-free designs have been reported[9,10]. All oligonucleotides in the designed structures are unique in sequence and readily open for a variety of modifications. Therefore, these DNA-based motifs can act as versatile templates for directing spatial arrangement of wide range of materials,[11] e.g. proteins,[12] carbon nanotubes,[13,14] and metal nanoparticles[15–19] with nanometer level accuracy. In addition, single-molecule chemical reactions can be conducted on an origami platform[20] and the formation of the origamis can be controlled using external trigger signals.[21]

The structural versatility and biocompatibility[8,22] of DNA origami nanostructures open up opportunities for effective, tunable and targeted transport of molecules into the cells. In principle, a single DNA origami structure could facilitate all functions necessary for drug delivery or docking molecules inside cells, since its configuration can be changed and the structure may include both cell-targeting ligands and spatially organized drug molecules or functionalized sites. Recently, cellular transfection of origamis and DNA nanoassemblies containing drugs such as DNA intercalator doxorubicin[23–25] has been demonstrated. In addition, a logic-gated DNA origami nanorobot that can release molecular payloads when triggered by cell surface proteins has been introduced.[26] There are also reports showing that DNA nanotubes,[27,28] DNA cages[29,30] and CpG-sequence-coated DNA origamis[31] could be taken up by cells. Due to its polar nature, DNA as such transfects poorly and in order to achieve an efficient uptake of DNA-based systems, cationic polymers or lipid formulations are commonly employed. However, efficient transfection of DNA, especially in the case of DNA origami structures,[32] is challenging and thus novel and versatile approaches are needed. One attractive option to enhance and improve the delivery of drugs and other functional DNA origamis would be to combine modularity of DNA structures with the ability of virus particles to encapsulate nucleic acids and target different tissue types (tropism). Several studies have already shown how viral nanoparticles and virus-like particles can be utilized as carriers in drug delivery and imaging.[33–36] Furthermore, drug-loaded DNA micelles have been applied as templates for virus capsid assembly when studying virus nanocarrier loading.[37] It has also been demonstrated that double-stranded DNA can be adopted as a template for virus capsid proteins to gain long tubular structures.[38]

In this communication we show how DNA origamis can be coated with virus capsid proteins in order to facilitate efficient cell transfection (see Figure 1).

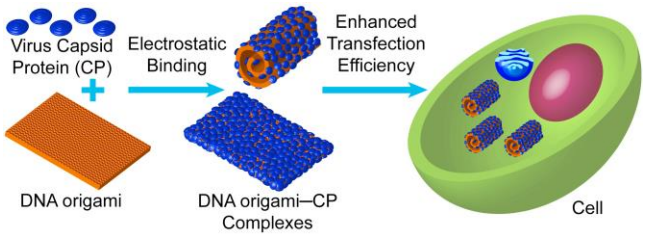

Figure 1. Self-assembly of DNA origamis with CPs. Origami-CP ratio controls the morphology of the resulting complex (wrapped or coated). Transfection efficiency increases with increasing concentration of CP.

For this, we employed ligated[39] rectangular DNA origami structures (72 nm x 92 nm)[1] to template the self-assembly of cowpea chlorotic mottle virus (CCMV) capsid proteins (CP). CCMV has become an important model system for chemical virology and is well-known to accept various synthetic and protein guest macromolecules inside the capsid.[40,41] CP dimers were isolated from the native virus particles by removing the viral (+)ssRNA genome. The purified CPs preserve their positively charged N-terminus, which allows the CPs to bind and self-assemble on the DNA origami nanostructures with high yields. Under the assembly conditions, oligomeric protein subunits are unable to form higher-order assembled structures (capsids, tubes etc.) without the DNA origami structure that functions as a template on which the capsid proteins assemble. Importantly, here the anisotropic shape of the origami can direct the assembly of the capsid proteins into structures that are significantly different from the native icosahedral symmetry. Binding of CPs on the origami structures and morphology of the resulting complexes were studied by gel electrophoretic mobility shift assay (EMSA), ethidium bromide (EthBr) fluorescence-quenching displacement assay and transmission electron microscopy (TEM). Furthermore, the ability of DNA origami–CP complexes to bind and transfect human cells was investigated. As shown by confocal microscopy and high content screening (HCS) microscopy,

transfection efficiency of DNA origami–CP complexes was 13 times higher compared to plain DNA origami structures.

DNA origamis and CCMV capsid protein dimers were prepared using standard annealing and calcium chloride precipitation procedures respectively (see the Supporting Information). The DNA origami–CP interaction was studied over a wide CP/DNA origami ratio and to achieve straightforward comparison between different samples and results gained with distinct methods, we define a ratio parameter γ, which is given by the number of CPs divided by the number of DNA base pairs (bp) in the sample solution ($n_{CP}/n_{DNA\ (bp)}$).

Electrostatic binding of CP on the negatively charged DNA origami surface was initially analyzed by gel electrophoretic mobility shift assay (EMSA) (Figure 2, top).

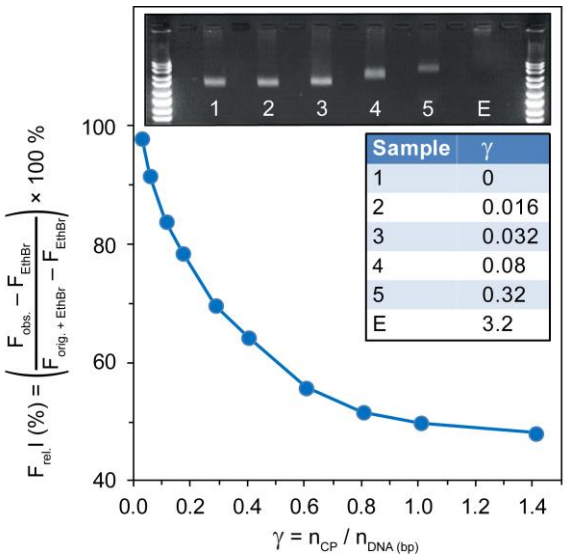

Figure 2. Gel electrophoretic mobility shift (top inset) and EthBr fluorescence-quenching displacement assays. Agarose gel EMSA of a constant amount of DNA origami complexed with increasing amounts of CP shows that DNA origami band shifts upward as a function of increasing CP concentration indicating binding (the gel visualized with EthBr). In sample E (excess CP) the amount of CP is drastically increased leading to the immobilization of the

complexes. A similar trend of binding can be seen in EthBr fluorescence assay, which shows how the DNA-bound EthBr fluorescence intensity decreases with increasing γ values.

Electrophoretic mobility of DNA origami decreases as CP binds on it and therefore EMSA samples were prepared by adding increasing amounts of CP to solutions with constant DNA origami concentration. With low amount of CP (γ = 0–0.032), the migration of DNA origami was unchanged. However, increasing the ratio to γ = 0.08 and further to 0.32, DNA origami migration was hindered indicating decrease in mobility and thus efficient binding of CPs to origamis. Furthermore, the migration was almost fully prevented at high ratios (γ = 3.2). These results strongly support that CPs bind to DNA origamis and the EMSA follows similar trend observed previously with CCMV CPs and linear dsDNA.[38] In addition to this experiment, electrostatic binding of CP without N-terminus (CPΔN), avidin and bovine serum albumin (BSA) to DNA origami structures was also studied (see the Supporting Information Figure S3). Results demonstrate that CP is unable to bind to DNA origami without the positively charged N-terminus and that the binding affinity of the proteins depends on their structure and isoelectric point: BSA (pI~4.8) does not bind at all and positively charged avidin (pI~10.5) induces a notable shift in the gel bands already at low γ ratios (γ = 0.032─0.08).

To complement the EMSA results, DNA origami–CP interaction was examined with EthBr fluorescence-quenching displacement assay (Figure 2, bottom). The assay determines how DNA-intercalating EthBr is released, or quenched, in the presence of CP by monitoring EthBr fluorescence intensity. The highest fluorescence intensity was measured from a solution containing only DNA origami (base pair concentration 170 nM) and EthBr (480 nM) (γ = 0). By adding CP to the solution, EthBr fluorescence intensity decreased as a function of increasing CP concentration and reached plateau at γ ~ 1. This was a clear indication of EthBr replacement with

CP on the surface of the DNA origami. The result further supports the formation of a complex between DNA origami structures and CPs.

Transmission electron microscopy (TEM) was conducted in order to visualize the morphology of the DNA origami–CP complexes (Figure 3, see the Supporting Information Figure S5 for additional images).

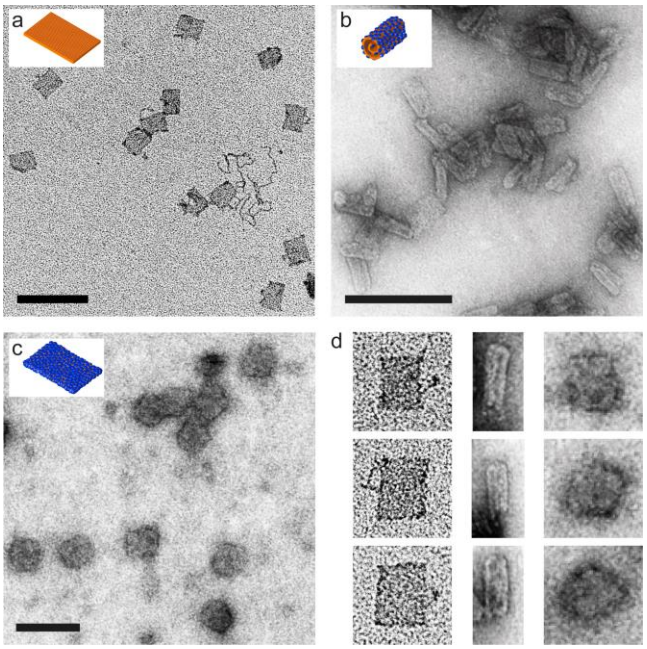

Figure 3. TEM micrographs from samples 1 (a), 4 (b) and 6 (c) showing how the morphology of the DNA origami–CP complexes changes while increasing the fraction of CP. Top left insets: schematic illustrations of three different morphologies (free rectangles, tubular and fully encapsulated. d) Magnified view of complexes presented in a (left), b (middle) and c (right). DNA origami concentration is constant in each sample, whereas CP concentration is increased so that γ grows as follows; (a) $\gamma = 0$, (b) $\gamma = 0.08$, (c) $\gamma = 0.64$. When the CP/DNA origami ratio is increased to $\gamma = 0.08$, capsid proteins start to attach onto the origami surfaces causing wrapping of the origamis. Further increase in the protein concentration leads to higher surface coverage of

CPs and thus to a complete encapsulation of open origami tiles ($\gamma = 0.64$). The scale bar in each figure is 200 nm.

Experiments were performed using the same γ values as in the EMSA measurement. Figure 3a presents plain DNA origami structures (sample 1, $\gamma = 0$) imaged with TEM. The expected rectangular shape of the origami can clearly be observed. When CP is added to the DNA origami solution, the capsid proteins bind to the origami surface and at a ratio of $\gamma = 0.08$ capsid proteins start to bend the DNA origami into tube-like conformations in large extends (Figure 3b, sample 4). Wrapping at a low protein concentration could be attributed to a high flexibility and significantly twisted natural shape of a rectangular origami in the solution due to the square lattice packing[42] (see also the Supporting Information Figure S1). Plausibly, twisting and bowing of the origamis can be further enhanced by positively charged CPs attached to the origami surface, since the positively charged residues could effectively reduce repulsion between the adjacent DNA helices. The length of the tubes was determined to be on average 80±3 nm, which matches well with a short side of a rectangular origami (72 nm) plus the thickness of CP coating (5 nm on both sides). In addition to perfect rolls, a small fraction of partly open origami structures were found, which made it evident that the complexes were formed from DNA origami substrates. When γ was further increased to 0.64, round and chunky complexes were observed instead of rolled structures (Figure 3c, sample 6). Because of the round but partly irregular shape of the complexes their size was challenging to quantify, but the diameter at the widest part for most structures was between 110–130 nm, which again matches well with the maximum cross-section of DNA origami (117 nm) supplemented with protein coat. Interestingly, in these samples the surface of complexes appeared to be granular when compared to bare DNA origamis. In addition, the open morphology increases the surface area of the origami and allows

maximal amount of CPs to bind on the origami surface. Taken together the observations indicate that the DNA template surface was completely covered with the CPs resulting in the encapsulation of the origamis.

The ability of DNA origami–CP complexes to enter cells was examined by confocal microscopy (see Figure 4a and 5).

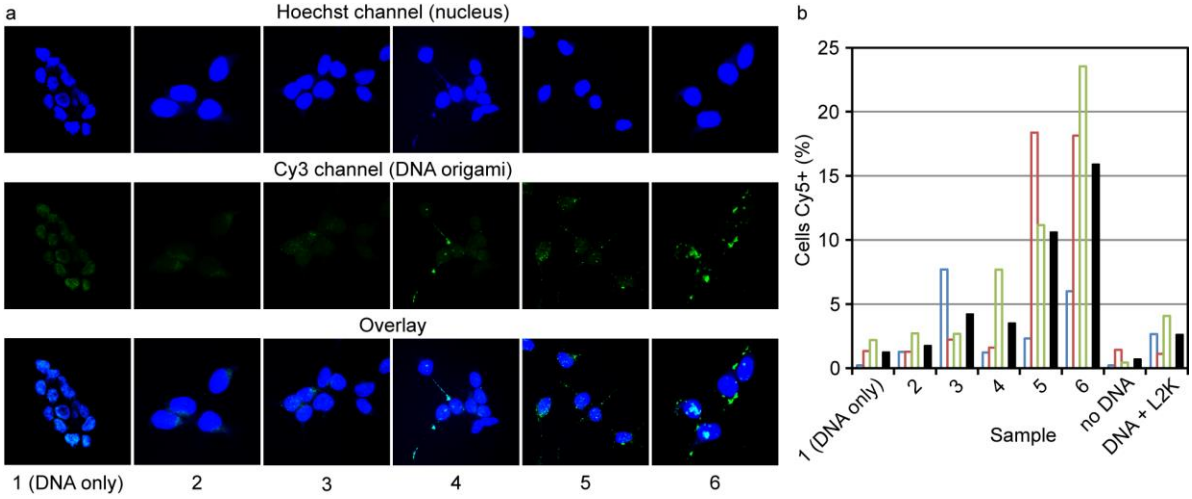

Figure 4. DNA origami transfection. a) Confocal microscopy (z-stack images) of HEK293 cells treated with DNA origami complexed with different amounts of CP. Top panel presents Hoechst channel (cell nuclei), middle panel Cy3 channel (DNA origamis) and bottom panel overlay of Hoechst and Cy3 channels b) Quantification of DNA origami–CP positive cells with HCS microscopy. Colored open bars indicate measurements from individual samples; black filled bars are calculated mean values of the triplicate samples.

Human embryonic kidney cells (HEK293) cells were incubated with Cy3-labeled origamis complexed with CP for 4 hours, after which aggregates of labeled origamis were observed within the fixed cells. The effect was clearly dependent on a CP concentration: only a few aggregates were seen in samples 1-3 ($\gamma = 0$, $\gamma = 0.016$, $\gamma = 0.032$), whereas samples 4-6 ($\gamma = 0.08$, $\gamma = 0.32$, $\gamma = 0.64$) displayed gradually increasing number and brightness of aggregates. The effect was

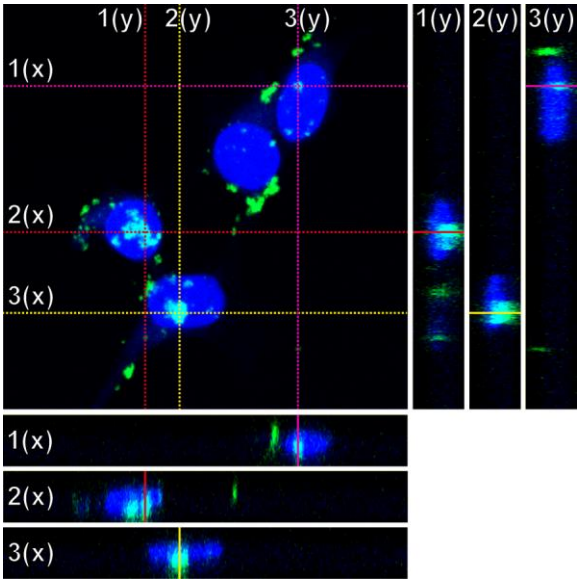

Figure 5. Confocal microscopy image (z-stack projection) of sample 6 with orthogonal cross sections (x and y views). Nuclear staining with Hoechst is shown in blue and Cy3-labeled DNA origami–CP complexes in green. z-stack projection image and orthogonal slices show that the Cy3-labeled origamis are in close proximity or within the cell nuclei, thus implying the intracellular localization of DNA origami–CP complexes.

quantified in a separate experiment using high content screening (HCS) microscopy of cells (transfected with GFP for visualization) incubated with Cy5-labeled DNA origami–CP complexes. Cy5-labeled samples 1 and 2 ($\gamma = 0$ and $\gamma = 0.016$) showed background levels of fluorescent positive cells, whereas samples 3–6 ($\gamma = 0.032$, $\gamma = 0.08$, $\gamma = 0.32$, $\gamma = 0.64$) clearly increased the fraction of labeled cells (see Figure 4b). Sample 6 showed on average 13-fold enhancement of transfection capability compared to sample 1 (DNA origami only). The transfection efficiency of DNA origami–CP complexes far exceeded that of the commercial Lipofectamine® 2000 (L2K) transfection reagent used as a positive control. During the time course of the experiment no significant cell toxicity was apparent, as examined by a methylthiazol tetrazolium (MTT) cytotoxicity assay (see the Supporting Information Figure S7).

Figure 5 shows in detail the co-localization of Cy3-labeled DNA origami–CP complexes and Hoechst-stained cell nuclei in sample 6, verifying the delivery of the complexes inside cells.

In summary, we have shown that DNA origami structures can interact with virus capsid proteins in a controllable way to form new nanostructures and that coating of origamis by these proteins can be exploited to significantly enhance delivery of DNA origamis into human cells. Interestingly, transfection efficiency could be gradually raised with increasing CP concentrations up to a level at which DNA origamis were completely covered by the capsid proteins. Although the present approach of using plant virus derived capsid proteins is not optimized and could probably be improved by adding cell targeting/penetrating ligands or by employing entirely different viruses, the obtained results conceivably make this self-assembly based method an excellent starting point for the development of diverse biomedical applications. The complete encapsulation gives a possibility to deliver multiple functionalized DNA origamis into cells and in this way use programmable combinations of specific drugs for attainable treatment procedures. In the future, organization of reactions inside the cell could be realized using modular docking sites on the origami,[43] similarly as earlier demonstrated for RNA-based assemblies[44].

ASSOCIATED CONTENT

Supporting Information

CanDo-simulated shape of a rectangular origami (without sidestrands) in a solution. Details of DNA origami formation, ligation and purification. Details of CP protein isolation and removal of N-terminus. Experimental details of determining the concentration of CPs and DNA origamis, EMSA, EthBr fluorescence quenching displacement assay, fluorescence spectroscopy, TEM imaging, cell culture treatment with DNA origami–CP complexes, confocal microscopy, fluorescence microscopy and HCS microscopy. Additional TEM micrographs of samples 1, 4 and 6. Fluorescence microscopy images of HEK293 cells treated with DNA origami–CP complex samples. Results of MTT cytotoxicity assay. This material is available free of charge via the Internet at http://pubs.acs.org.

AUTHOR INFORMATION

Corresponding Author

Mauri.Kostiainen@aalto.fi

Author Contributions

The manuscript was written through contributions of all authors. All authors have given approval to the final version of the manuscript.

Notes

The authors declare no competing financial interests.

ACKNOWLEDGMENT

J.M., V.L. and M.A.K. acknowledge support through the Emil Aaltonen Foundation and the Academy of Finland (grants 267497, 273645 and 263504), A.-P. E. through the Finnish National Graduate School in Nanoscience (NGS-Nano) and M.J.F. through the Academy of Finland and the Sigrid Jusélius Foundation. This work was supported by the Academy of Finland through its Centers of Excellence Program (projects No. 251748, No. 135000, No. 141039, No. 263347 and No. 272490). This work made use of the Aalto University Nanomicroscopy Centre (Aalto NMC) and the Light Microscopy Unit at Institute of Biotechnology (University of Helsinki).

REFERENCES

(1) Rothemund, P. W. K. Nature 2006, 440, 297–302.

(2) Andersen, E. S.; Dong, M.; Nielsen, M. M.; Jahn, K.; Subramani, R.; Mamdouh, W.; Golas, M. M.; Sander, B.; Stark, H.; Oliveira, C. L. P.; Pedersen, J. S.; Birkedal, V.; Besenbacher, F.; Gothelf, K. V; Kjems, J. Nature 2009, 459, 73–76.

(3) Douglas, S. M.; Dietz, H.; Liedl, T.; Högberg, B.; Graf, F.; Shih, W. M. Nature 2009, 459, 414–418.

(4) Dietz, H.; Douglas, S. M.; Shih, W. M. Science 2009, 325, 725–730.

(5) Liedl, T.; Högberg, B.; Tytell, J.; Ingber, D. E.; Shih, W. M. Nat. Nanotechnol. 2010, 5, 520–524.

(6) Linko, V.; Dietz, H. Curr. Opin. Biotechnol. 2013, 24, 555–561.

(7) Han, D.; Pal, S.; Nangreave, J.; Deng, Z.; Liu, Y.; Yan, H. Science 2011, 332, 342–346.

(8) Castro, C. E.; Kilchherr, F.; Kim, D.-N.; Shiao, E. L.; Wauer, T.; Wortmann, P.; Bathe, M.; Dietz, H. Nat. Methods 2011, 8, 221–229.

(9) Wei, B.; Dai, M.; Yin, P. Nature 2012, 485, 623–626.

(10) Ke, Y.; Ong, L. L.; Shih, W. M.; Yin, P. Science 2012, 338, 1177–1183.

(11) Seeman, N. C. Nano Lett. 2010, 10, 1971–1978.

(12) Kuzyk, A.; Laitinen, K. T.; Törmä, P. Nanotechnology 2009, 20, 235305.

(13) Maune, H. T.; Han, S.-P.; Barish, R. D.; Bockrath, M.; Goddard III, W. A.; Rothemund, P. W. K.; Winfree, E. Nat. Nanotechnol. 2010, 5, 61–66.

(14) Eskelinen, A.-P.; Kuzyk, A.; Kaltiaisenaho, T. K.; Timmermans, M. Y.; Nasibulin, A. G.; Kauppinen, E. I.; Törmä, P. Small 2011, 7, 746–750.

(15) Hung, A. M.; Micheel, C. M.; Bozano, L. D.; Osterbur, L. W.; Wallraff, G. M.; Cha, J. N. Nat. Nanotechnol. 2010, 5, 121–126.

(16) Pal, S.; Deng, Z.; Ding, B.; Yan, H.; Liu, Y. Angew. Chem. Int. Ed. 2010, 49, 2700–2704.

(17) Kuzyk, A.; Schreiber, R.; Fan, Z.; Pardatscher, G.; Roller, E.-M.; Högele, A.; Simmel, F. C.; Govorov, A. O.; Liedl, T. Nature 2012, 483, 311–314.

(18) Eskelinen, A.-P.; Moerland, R. J.; Kostiainen, M. A.; Törmä, P. Self-Assembled Silver Nanoparticles in a Bow-Tie Antenna Configuration. Small [Online early access].

DOI:10.1002/smll.201302046. Published Online: Nov 11, 2013. http://onlinelibrary.wiley.com/doi/10.1002/smll.201302046/full (accessed Dec 17, 2013).

(19) Zheng, J.; Constantinou, P. E.; Micheel, C.; Alivisatos, A. P.; Kiehl, R. A.; Seeman, N. C. Nano Lett. 2006, 6, 1502–1504.

(20) Voigt, N. V.; Tørring, T.; Rotaru, A.; Jacobsen, M. F.; Ravnsbæk, J. B.; Subramani, R.; Mamdouh, W.; Kjems, J.; Mokhir, A.; Besenbacher, F.; Gothelf, K. V. Nat. Nanotechnol. 2010, 5, 200–203.

(21) Eskelinen, A.-P.; Rosilo, H.; Kuzyk, A.; Törmä, P.; Kostiainen, M. A. Small 2012, 8, 2016–2020.

(22) Mei, Q.; Wei, X.; Su, F.; Liu, Y.; Youngbull, C.; Johnson, R.; Lindsay, S.; Yan, H.; Meldrum, D. Nano Lett. 2011, 11, 1477–1482.

(23) Jiang, Q.; Song, C.; Nangreave, J.; Liu, X.; Lin, L.; Qiu, D.; Wang, Z.-G.; Zou, G.; Liang, X.; Yan, H.; Ding, B. J. Am. Chem. Soc. 2012, 134, 13396–13403.

(24) Zhao, Y.-X.; Shaw, A.; Zeng, X.; Benson, E.; Nyström, A. M.; Högberg, B. ACS Nano 2012, 6, 8684–8691.

(25) Wu, C.; Han, D.; Chen, T.; Peng, L.; Zhu, G.; You, M.; Qiu, L.; Sefah, K.; Zhang, X.; Tan, W. J. Am. Chem. Soc. 2013, 135, 18644–18650.

(26) Douglas, S. M.; Bachelet, I.; Church, G. M. Science 2012, 335, 831–834.

(27) McLaughlin, C. K.; Hamblin, G. D.; Hänni, K. D.; Conway, J. W.; Nayak, M. K.; Carneiro, K. M. M.; Bazzi, H. S.; Sleiman, H. F. J. Am. Chem. Soc. 2012, 134, 4280–4286.

(28) Ko, S.-H.; Liu, H.; Chen, Y.; Mao, C. Biomacromolecules 2008, 9, 3039–3043.

(29) Walsh, A. S.; Yin, H.; Erben, C. M.; Wood, M. J. A.; Turberfield, A. J. ACS Nano 2011, 5, 5427–5432.

(30) Li, J.; Pei, H.; Zhu, B.; Liang, L.; Wei, M.; He, Y.; Chen, N.; Li, D.; Huang, Q.; Fan, C. ACS Nano 2011, 5, 8783–8789.

(31) Schüller, V. J.; Heidegger, S.; Sandholzer, N.; Nickels, P. C.; Suhartha, N. A.; Endres, S.; Bourquin, C.; Liedl, T. ACS Nano 2011, 5, 9696–9702.

(32) Okholm, A. H.; Nielsen, J. S.; Vinther, M.; Sørensen, R. S.; Schaffert, D.; Kjems, J. Quantification of cellular uptake of DNA nanostructures by qPCR. Methods[Online early access]. DOI:10.1016/j.ymeth.2014.01.013. Published Online: Jan 25, 2014. http://www.sciencedirect.com/science/article/pii/S1046202314000231# (accessed Feb 5, 2013).

(33) Brasch, M.; de la Escosura, A.; Ma, Y.; Uetrecht, C.; Heck, A. J. R.; Torres, T.; Cornelissen, J. J. L. M. J. Am. Chem. Soc. 2011, 133, 6878–6881.

(34) Zeng, Q.; Wen, H.; Wen, Q.; Chen, X.; Wang, Y.; Xuan, W.; Liang, J.; Wan, S. Biomaterials 2013, 34, 4632–4642.

(35) Yildiz, I.; Shukla, S.; Steinmetz, N. F. Curr. Opin. Biotechnol. 2011, 22, 901–908.

(36) Ma, Y.; Nolte, R. J. M.; Cornelissen, J. J. L. M. Adv. Drug Deliv. Rev. 2012, 64, 811–825.

(37) Kwak, M.; Minten, I. J.; Anaya, D.-M.; Musser, A. J.; Brasch, M.; Nolte, R. J. M.; Müllen, K.; Cornelissen, J. J. L. M.; Herrmann, A. J. Am. Chem. Soc. 2010, 132, 7834–7835.

(38) Mukherjee, S.; Pfeifer, C. M.; Johnson, J. M.; Liu, J.; Zlotnick, A. J. Am. Chem. Soc. 2006, 128, 2538–2539.

(39) O'Neill, P.; Rothemund, P. W. K.; Kumar, A.; Fygenson, D. K. Nano Lett. 2006, 6, 1379–1383.

(40) Douglas, T.; Young, M. Nature 1998, 393, 152–155.

(41) Young, M.; Willits, D.; Uchida, M.; Douglas, T. Annu. Rev. Phytopathol. 2008, 46, 361–384.

(42) Ke, Y.; Douglas, S. M.; Liu, M.; Sharma, J.; Cheng, A.; Leung, A.; Liu, Y.; Shih, W. M.; Yan, H. J. Am. Chem. Soc. 2009, 131, 15903–15908.

(43) Simmel, F. C. Curr. Opin. Biotechnol. 2012, 23, 516–521.

(44) Delebecque, C. J.; Lindner, A. B.; Silver, P. A.; Aldaye, F. A. Science 2011, 333, 470–474.

TOC